Supplementary Online Content

Shankar GM, Francis JM, Rinne ML, et al. Rapid Intraoperative Molecular Characterization of Glioma. *JAMA Oncology*. Published online May 14, 2015. doi:10.1001/jamaoncol.2015.0917.

eMethods. Supplementary Methods
eFigure 1. Modified oligonucleotides selectively block exponential PCR amplification of wild-type alleles. Peptide nucleic acid (PNA) oligonucleotides were designed to target wild-type alleles of (a) IDH1 R132, (b) TERT C228 and TERT C250. Genomic extracts were obtained from HCC1143 lymphocytes (wt), wild-type HCC1954 lymphocytes (1954), BT142 primary glioma cell line with hemizygous IDH1 R132H mutation, primary glioma cell line LN428 with TERT C228T mutation and primary glioma cell line LN443 with TERT C250T mutation. PNA oligonucleotides have dose-dependent effects in selectively blocking wild-type allele amplification, while allowing for PCR amplification of mutant alleles.
eFigure 2. Sanger sequencing validation of positive and negative control genomic extracts. (a) IDH1 and (b) TERT promoter amplicons were confirmed by Sanger sequencing. PCR products were generated in the absence of PNA oligonucleotide blockers.
eFigure 3. Locked nucleic acid probes are specific for detection of mutant alleles. Locked nucleic acid (LNA) probes were designed for targeting (a) IDH1 R132H, (b) TERT C228T, or (c) TERT C250T. LNA probes selectively detect mutant alleles, but not wild-type (wt) alleles. Genomic DNA from BT142, LN428, or LN443 was diluted serially in wild-type genomic extract and tested in duplicate. These experiments were performed in the absence of modified PNA oligonucleotides. Corresponding run temperature plot reveals detection of 100% to 0.1% allelic fraction of IDH1 R132H in 36 to 46 minutes, TERT C228T in 29 to 39 minutes, and TERT C250T in 30 to 39 minutes.
eFigure 4. Quantitative analysis allows for gross estimation of tumor purity. OperaGen performed in the presence of modified PNA oligonucleotides allows for gross estimation of tumor purity when tumor genomic extract from positive control cell lines (red squares for TERT C228T from LN428, green triangles for TERT C250T from LN443, and blue diamonds for IDH1 R132H from BT142) is serially diluted in wild-type genomic extract. The amount of positive control extract (in ng on logarithmic scale) contained within the serial dilution is plotted with respect to the threshold cycle. Data are fitted by exponential approximation.
eFigure 5. Difficulty of intraoperative confirmation of diffuse glioma affects surgical management. Analysis of the surgical management of 72 new diagnoses of WHO Grade II gliomas to Brigham and Women's Hospital between 2009-2014 revealed that the intraoperative frozen section analysis was inconclusive for

glioma in 39% (pink) of cases and that a staged craniotomy approach was performed in 12% of cases (red). Black shading in the outer ring denotes cases that may have benefitted from intraoperative molecular testing.

eFigure 6. TERT promoter amplicon characterization by deep sequencing in non-scoring and discordant samples noted in Figure 1a. PCR amplicons of the TERT promoter were generated in the samples that were discordant between molecular characterization and clinical pathologic diagnosis and subjected to high depth sequencing (mean depth 250,000x). Positive controls for TERT C228T and TERT C250T were also run in parallel. Fraction of mutant alleles detected by high depth sequencing is displayed in white text within respective TERT mutations. The TERT C250T mutation was observed at an allelic fraction of ~10% by MiSeq in the one sample that was characterized as diffuse astrocytoma, but noted to have a co-mutation of IDH1 and TERT C250T by OperaGen. The other seven samples in which no TERT promoter mutations were observed by OperaGen were also wild-type by high depth sequencing of the amplicon.

eFigure 7. Prognosis of glioma correlates with IDH1 and TERT promoter genotype. (a) Time to treatment failure, or progression and (b) overall survival was plotted with respect to IDH1 and TERT promoter mutation status for patients analyzed in Figure 1a. Presence of IDH1 mutation regardless of TERT promoter status predicts longer time to treatment failure and overall survival compared to IDH1 wildtype ($p < 0.01$, log rank test). IDH1 and TERT promoter co-mutated gliomas (blue line) demonstrated no difference in time to treatment failure, but were noted to have statistically significant longer overall survival ($p = 0.036$) when compared to IDH1 mutant, TERT promoter wildtype gliomas (green line).

eFigure 8. Detection and discrimination of glioma-specific IDH1 mutations in a multiplexed reaction. 5' Nuclease LNA oligonucleotides were conjugated to VIC-fluorophore and designed to specifically detect (a, top right) IDH1 R132C, (a, bottom left) IDH1 R132G, (a, bottom right) IDH1 R132S, or (b, right) IDH1 R132L. Non-specific fluorescence was not detected by the FAM-conjugated probe directed against the IDH1 R132H variant (a, top left and b, left). Frozen WHO grade II glioma specimens from Figure 1b were used in the analysis of panel a. IDH1 R132H positive control from BT142 cell extract and separately obtained FFPE specimens from gliomas bearing the IDH1 R132L were used for validation of the probe in panel b. All 5'Nuclease probes were combined in a single reaction, each at a final concentration of 250 nM, for the multiplexed detection and discrimination of these IDH1 variants, but the specificity of each probe was initially tested separately. All samples were run in duplicate.

eFigure 9. Sensitivity and specificity analysis of OperaGen results compared to final pathologic diagnosis. (a) Assessment of OperaGen false positive rate in a third cohort representing 50 frozen GBM specimens. Two samples were noted by OperaGen to have IDH1 R132H and 39 samples were noted to have either TERT C228T or TERT C250T. The prevalence of non-scoring specimens in this cohort is the similar to the ratio of non-scoring GBM specimens in Figure 1a ($p > 0.05$ by Fisher's exact test). (b) Expanded heatmap from Figure 1a demonstrating individual IDH1 R132H, TERT C228T and TERT C250T mutations

for each glioma specimen. OperaGen sensitivity and specificity for predicting (b) oligodendrogliomas, diffuse astrocytomas, oligoastrocytomas or IDH1 mutant glioblastomas or (d) primary glioblastoma with 95% confidence intervals in parentheses.

eFigure 10. Proposed workflow of intraoperative OperaGen analysis of biopsy specimen. The specimen would be immediately placed in lysis buffer and incubated at 55˚C en route to the frozen pathology lab. DNA extraction is completed with magnetic beads. This sample is applied to a plate already containing the optimized mastermix to detect IDH1 R132 variants, TERT C228T or TERT C250T with respective controls.Flow of information through the different phases of the review

eTable 1. List of primers, detection probes and modified oligonucleotide blockers. Modified locked nucleic acids are indicated by a preceeding "+".

eTable 2. List of non-glioma biopsies analyzed by OperaGen. Fourteen non-glioma biopsy specimens were analyzed for IDH1 and TERT promoter variants by OperaGen. None of these were noted to be positive for variants in either gene.

eTable 3. Intraoperative histologic analysis of 14 stereotactic glioma biopsies. The intraoperative histologic analysis and final histologic diagnosis are presented for the 14 biopsy cases presented in Figure 2b (preserving the order from left to right). The number of biopsy cores obtained for each patient is listed in the second column.

This supplementary material has been provided by the authors to give readers additional information about their work.

SUPPLEMENTARY METHODS

Quantitative PCR assay

5' Nuclease probes against mutant alleles and corresponding PNA oligonucleotide blockers against wild-type alleles were designed to detect IDH1 R132H, R132C, R132G, R132S and R132L and *TERT* promoter mutations on chromosome 5 at positions 1,295,228 and 1,295,250 based on human genome reference version 19 (referred to hereafter as *TERT* C228T or *TERT* C250T) (eTable 1). Optimal sensitivity was achieved through the use of two distinct *TERT* wild-type blocking oligonucleotides. *TERT* assays were performed using Kapa Biosystems 2G Fast PCR polymerase in buffer A with enhancer and the *IDH1* assays were run in the ABI Taqman Gene Expression mastermix containing oligonucleotide concentrations as outline in eTable 1. To ensure the integrity of the assay, every qPCR reaction was run in duplicate and included positive controls from BT142, LN428, LN443 glioma cell lines and negative controls from wildtype lymphocyte genomic extracts. To account for batch variability, a run-specific threshold was set based on the controls. The qPCR reactions were run on a QuantStudio6 instrument (Applied Biosystems), with a time/cycle of 58.2s/cycle, respectively. The lid was preheated and PCR cycling times were 95˚C for 3 minutes followed by 50 cycles at 95˚ for 10 seconds and 63.5˚C for 20 seconds. We minimized the ramp times by setting the heating algorithm to half the reaction volume. Reactions were performed with 25ng of whole genomic extract.

Development and optimization of rapid genotyping assay

One challenge of detecting mutant alleles in brain biopsies with infrequent tumor cells is competition for PCR reagents by wild-type alleles from surrounding normal cells. To address this, PNA oligonucleotides, which cannot be digested by 5' exonuclease activity or used as a primer for extension by DNA polymerase, were used to block the amplification of wild-type alleles (eFigure 1). At the same time, high mutant allele specificity was achieved through the use of LNAs, where a chemically synthesized ribose moiety stabilized by an additional covalent bond is incorporated into the detection probe in order to optimize hybridization characteristics and minimize non-specific binding to wild-type alleles. *TERT* promoter and *IDH1* control templates were validated by Sanger sequencing (eFigure 2). The assay design allowed for simultaneous parallel detection of *IDH1* and *TERT* promoter mutations. In this optimized assay, we could detect serial dilutions representing 0.1%-10% of positive control genomic extracts diluted in negative control extracts (eFigure 3). Estimation of tumor purity was extrapolated from standard curves (eFigure 4). For validation by next generation sequencing, PCR amplicons were generated for these regions and subjected to high depth sequencing by MiSeq (Illumina). Sequences were aligned by standard methods and were manually reviewed by Integrated Genome Viewer with allelic fraction threshold of 5%.

Tumor specimens

Case records were reviewed and glioma specimens were obtained under approval of the Institutional Review Boards at Dana-Farber Cancer Institute and Massachusetts General Hospital.

Control genomic templates

IDH1 R132H control template was isolated from BT142 cells (ATCC)[33]. The *TERT* C228T and *TERT* C250T control templates were isolated from glioma cell lines LN428 and LN443, respectively. DNA was extracted from cell pellets and formalin-fixed, paraffin-embedded (FFPE) specimens using the QiaAMP kit, and from fresh intraoperative specimens by a modified ChargeSwitch protocol (Invitrogen). Briefly, tissue was snap frozen, thawed and pulverized by a sterile pestle before the addition of 1 mL of warmed lysis buffer containing 100 units of Proteinase K. The tissue was incubated at 55˚C for 3 minutes with intermittent mixing prior to addition of 0.2 mL of purification buffer and 0.04 mL of magnetic ChargeSwitch beads. The beads were incubated with lysed tissue for 1 min, washed two times in 1 mL of wash buffer and eluted in 0.05 mL of elution buffer. Concentration of genomic extract was quantified by PicoGreen dsDNA assay (Life Technologies).

eFigure 1

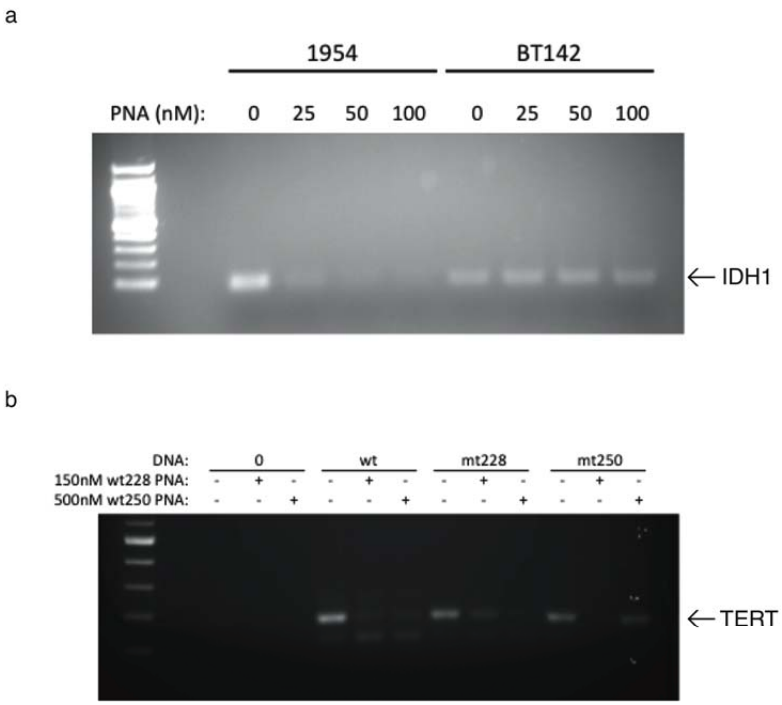

eFigure 1. Modified oligonucleotides selectively block exponential PCR amplification of wild-type alleles. Peptide nucleic acid (PNA) oligonucleotides were designed to target wild-type alleles of (a) IDH1 R132, (b) *TERT* C228 and *TERT* C250. Genomic extracts were obtained from HCC1143 lymphocytes (wt), wild-type HCC1954 lymphocytes (1954), BT142 primary glioma cell line with hemizygous IDH1 R132H mutation, primary glioma cell line LN428 with *TERT* C228T mutation and primary glioma cell line LN443 with *TERT* C250T mutation. PNA oligonucleotides have dose-dependent effects in selectively blocking wild-type allele amplification, while allowing for PCR amplification of mutant alleles.

eFigure 2

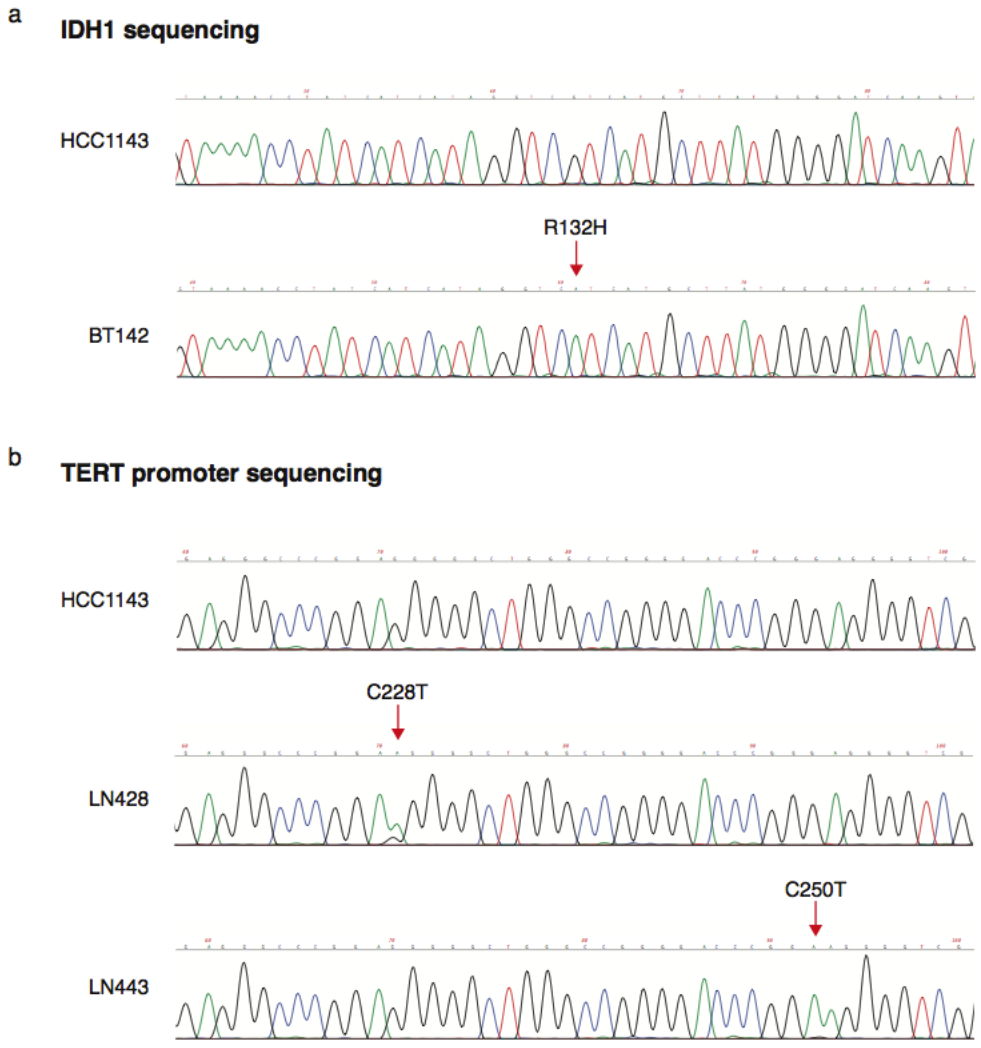

eFigure 2. Sanger sequencing validation of positive and negative control genomic extracts. (a) *IDH1* and (b) *TERT* promoter amplicons were confirmed by Sanger sequencing. PCR products were generated in the absence of PNA oligonucleotide blockers.

eFigure 3

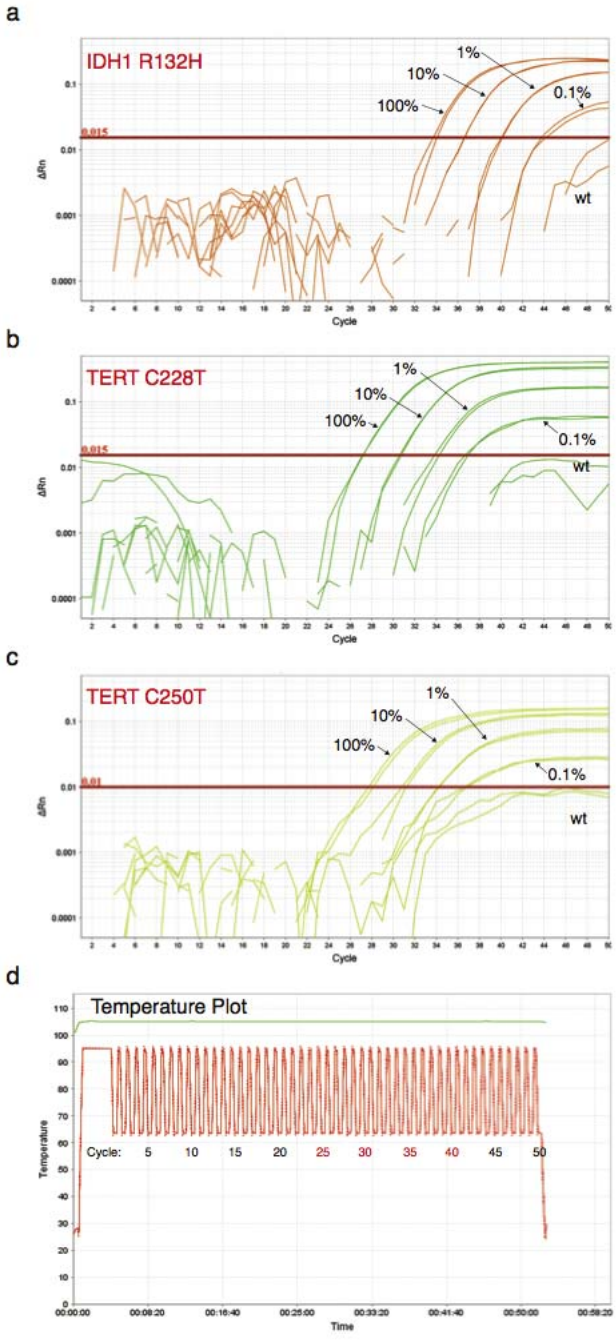

eFigure 3. Locked nucleic acid probes are specific for detection of mutant alleles. Locked nucleic acid (LNA) probes were designed for targeting (a) IDH1 R132H, (b) *TERT* C228T, or (c) *TERT* C250T. LNA probes selectively detect mutant alleles, but not wild-type (wt) alleles. Genomic DNA from BT142, LN428, or LN443 was diluted serially in wild-type genomic extract and tested in duplicate. These experiments were performed in the absence of modified PNA oligonucleotides. Corresponding run temperature plot reveals detection of 100% to 0.1% allelic fraction of IDH1 R132H in 36 to 46 minutes, *TERT* C228T in 29 to 39 minutes, and *TERT* C250T in 30 to 39 minutes.

eFigure 4

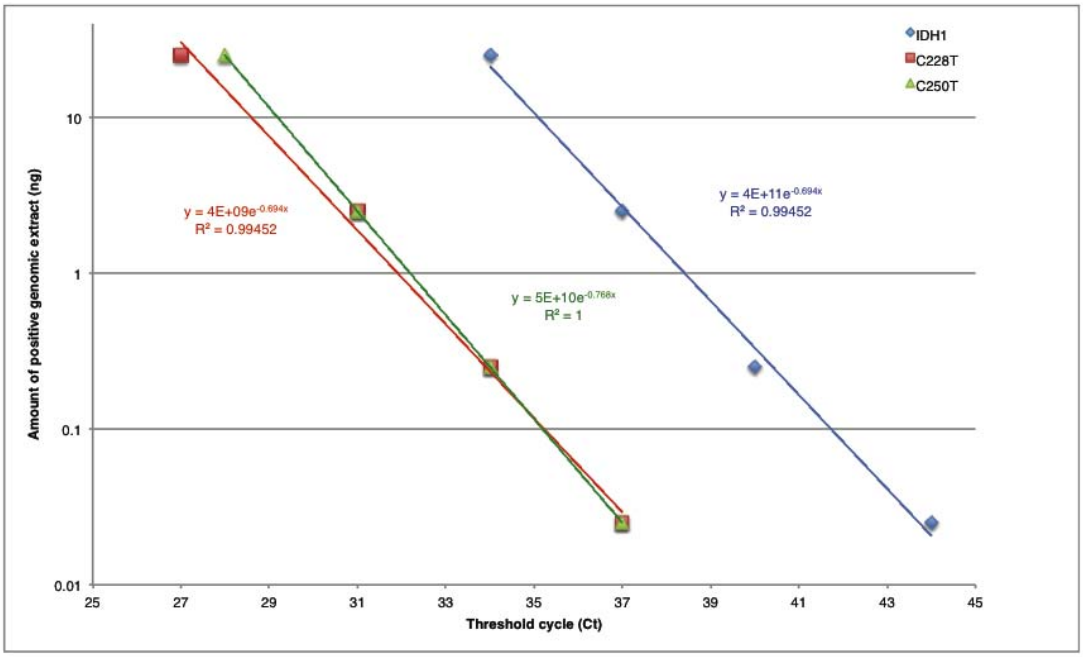

eFigure 4. Quantitative analysis allows for gross estimation of tumor purity. OperaGen performed in the presence of modified PNA oligonucleotides allows for gross estimation of tumor purity when tumor genomic extract from positive control cell lines (red squares for *TERT* C228T from LN428, green triangles for *TERT* C250T from LN443, and blue diamonds for IDH1 R132H from BT142) is serially diluted in wild-type genomic extract. The amount of positive control extract (in ng on logarithmic scale) contained within the serial dilution is plotted with respect to the threshold cycle. Data are fitted by exponential approximation.

eFigure 5

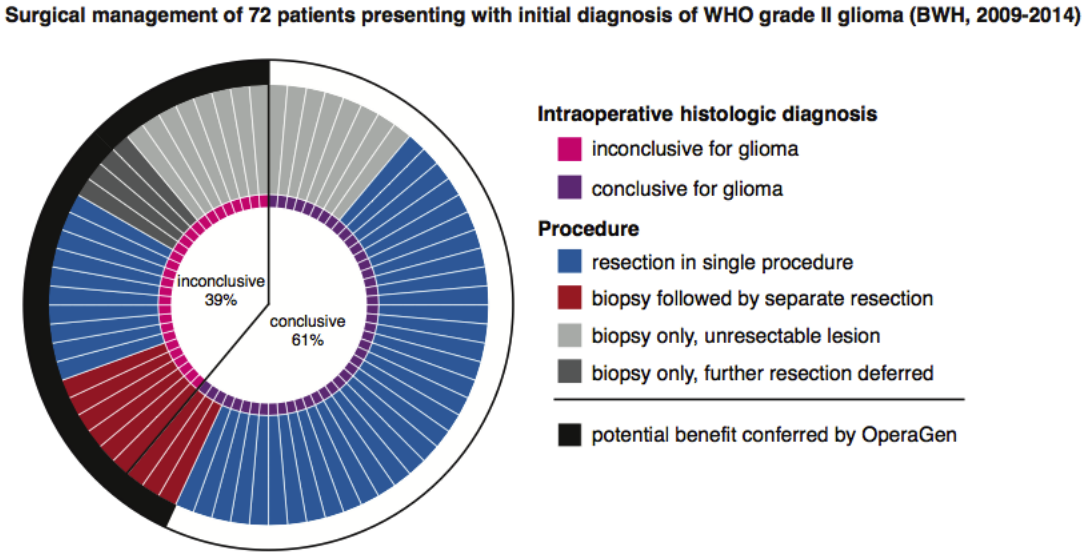

eFigure 5. Difficulty of intraoperative confirmation of diffuse glioma affects surgical management. Analysis of the surgical management of 72 new diagnoses of WHO Grade II gliomas to Brigham and Women's Hospital between 2009-2014 revealed that the intraoperative frozen section analysis was inconclusive for glioma in 39% (pink) of cases and that a staged craniotomy approach was performed in 12% of cases (red). Black shading in the outer ring denotes cases that may have benefitted from intraoperative molecular testing.

eFigure 6

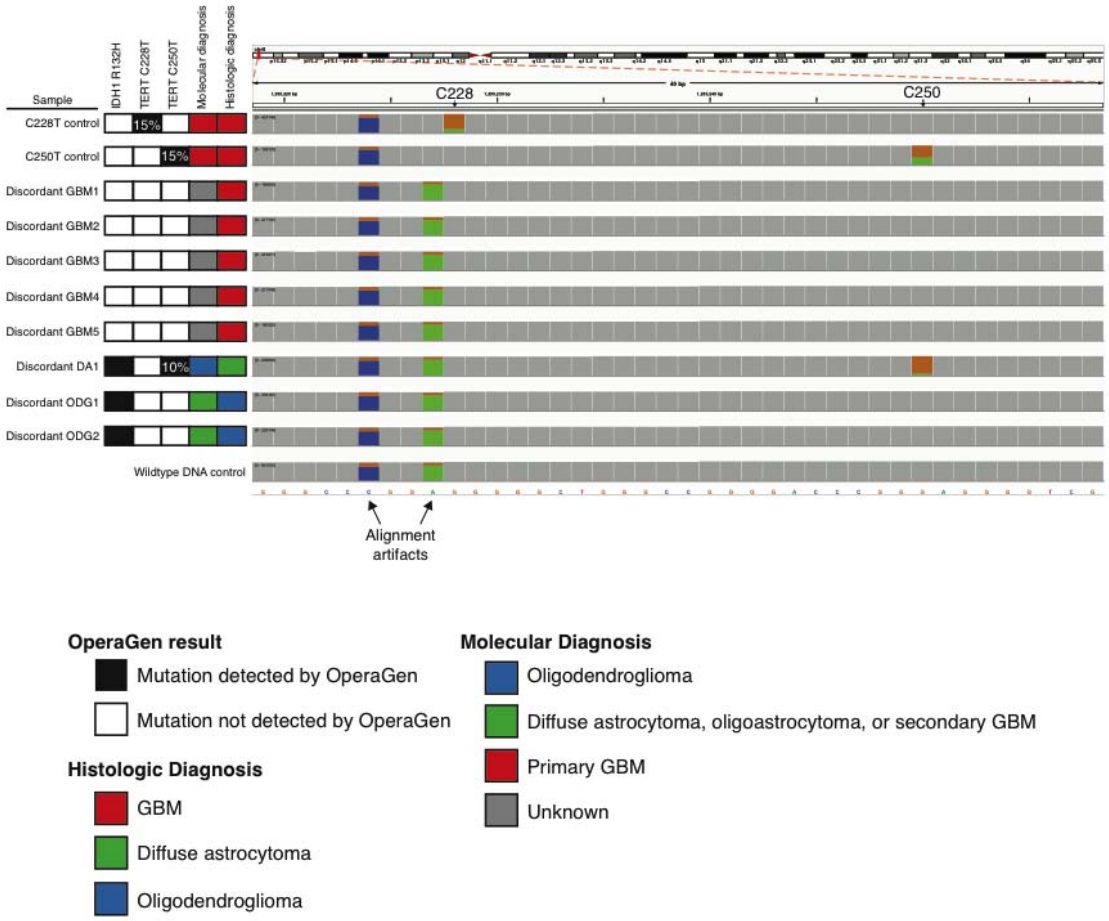

eFigure 6. *TERT* promoter amplicon characterization by deep sequencing in non-scoring and discordant samples noted in Figure 1a. PCR amplicons of the TERT promoter were generated in the samples that were discordant between molecular characterization and clinical pathologic diagnosis and subjected to high depth sequencing (mean depth 250,000x). Positive controls for *TERT* C228T and *TERT* C250T were also run in parallel. Fraction of mutant alleles detected by high depth sequencing is displayed in white text within respective *TERT* mutations. The *TERT* C250T mutation was observed at an allelic fraction of ~10% by MiSeq in the one sample that was characterized as diffuse astrocytoma, but noted to have a co-mutation of *IDH1* and *TERT* C250T by OperaGen. The other seven samples in which no *TERT* promoter mutations were observed by OperaGen were also wild-type by high depth sequencing of the amplicon.

eFigure 7

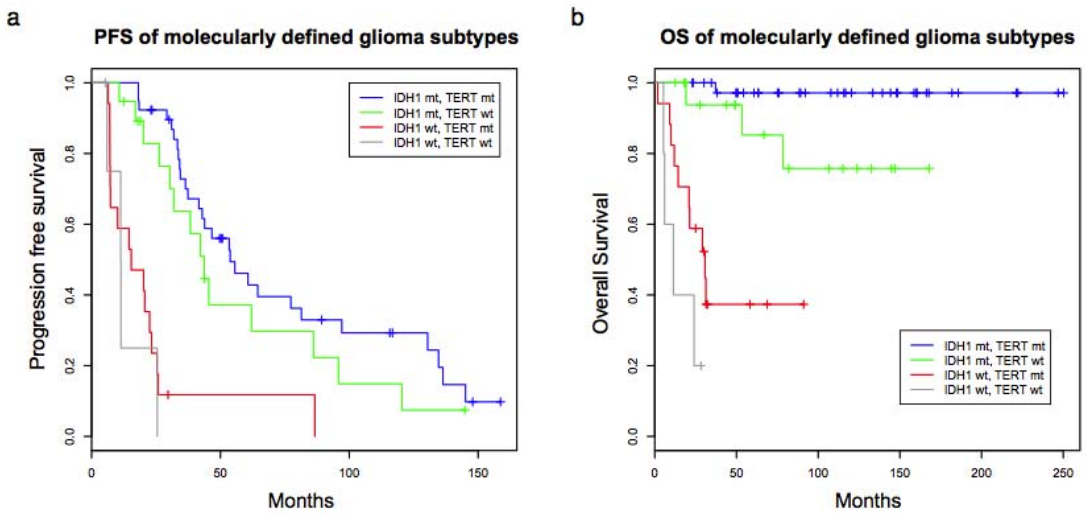

eFigure 7. Prognosis of glioma correlates with *IDH1* and *TERT* promoter genotype. (a) Time to treatment failure, or progression and (b) overall survival was plotted with respect to *IDH1* and *TERT* promoter mutation status for patients analyzed in Figure 1a. Presence of *IDH1* mutation regardless of *TERT* promoter status predicts longer time to treatment failure and overall survival compared to *IDH1* wildtype ($p < 0.01$, log rank test). *IDH1* and *TERT* promoter co-mutated gliomas (blue line) demonstrated no difference in time to treatment failure, but were noted to have statistically significant longer overall survival ($p = 0.036$) when compared to *IDH1* mutant, *TERT* promoter wildtype gliomas (green line).

eFigure 8

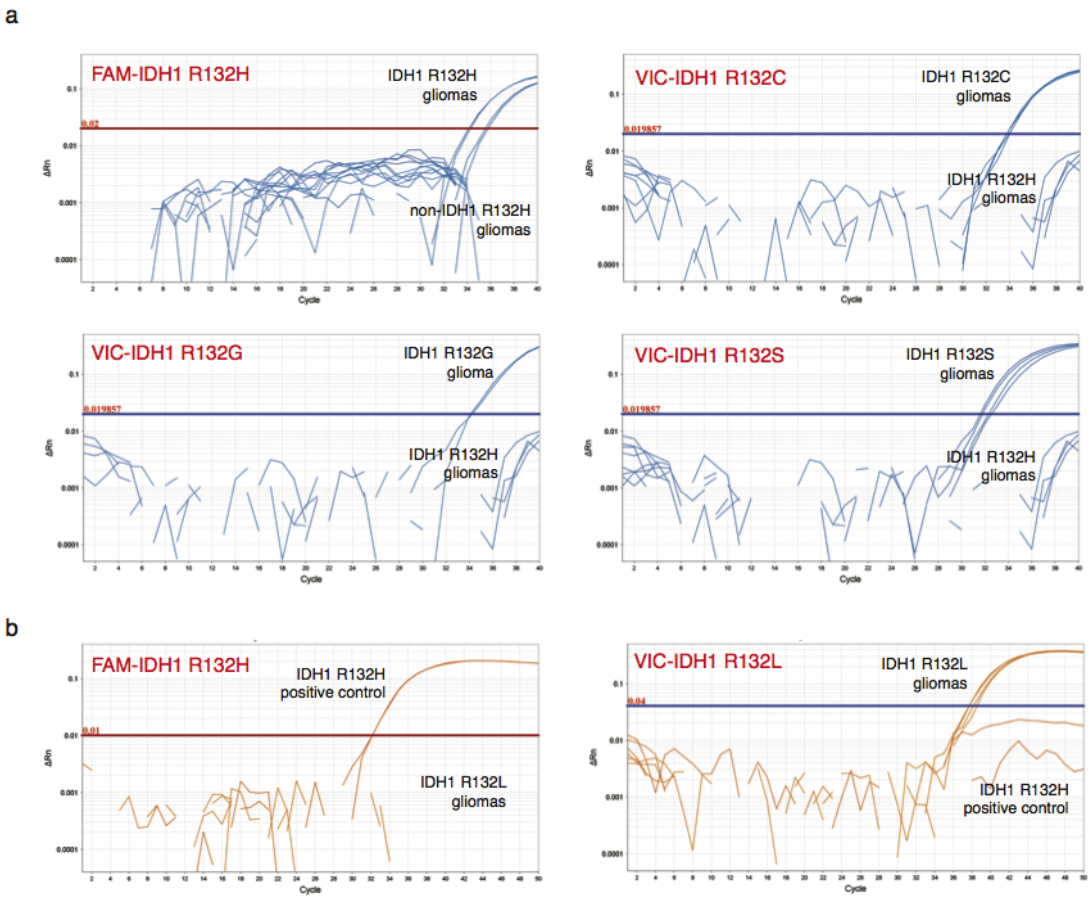

eFigure 8. Detection and discrimination of glioma-specific IDH1 mutations in a multiplexed reaction. 5' Nuclease LNA oligonucleotides were conjugated to VIC-fluorophore and designed to specifically detect (a, top right) IDH1 R132C, (a, bottom left) IDH1 R132G, (a, bottom right) IDH1 R132S, or (b, right) IDH1 R132L. Non-specific fluorescence was not detected by the FAM-conjugated probe directed against the IDH1 R132H variant (a, top left and b, left). Frozen WHO grade II glioma specimens from Figure 1b were used in the analysis of panel a. IDH1 R132H positive control from BT142 cell extract and separately obtained FFPE specimens from gliomas bearing the IDH1 R132L were used for validation of the probe in panel b. All 5'Nuclease probes were combined in a single reaction, each at a final concentration of 250 nM, for the multiplexed detection and discrimination of these *IDH1* variants, but the specificity of each probe was initially tested separately. All samples were run in duplicate.

eFigure 9

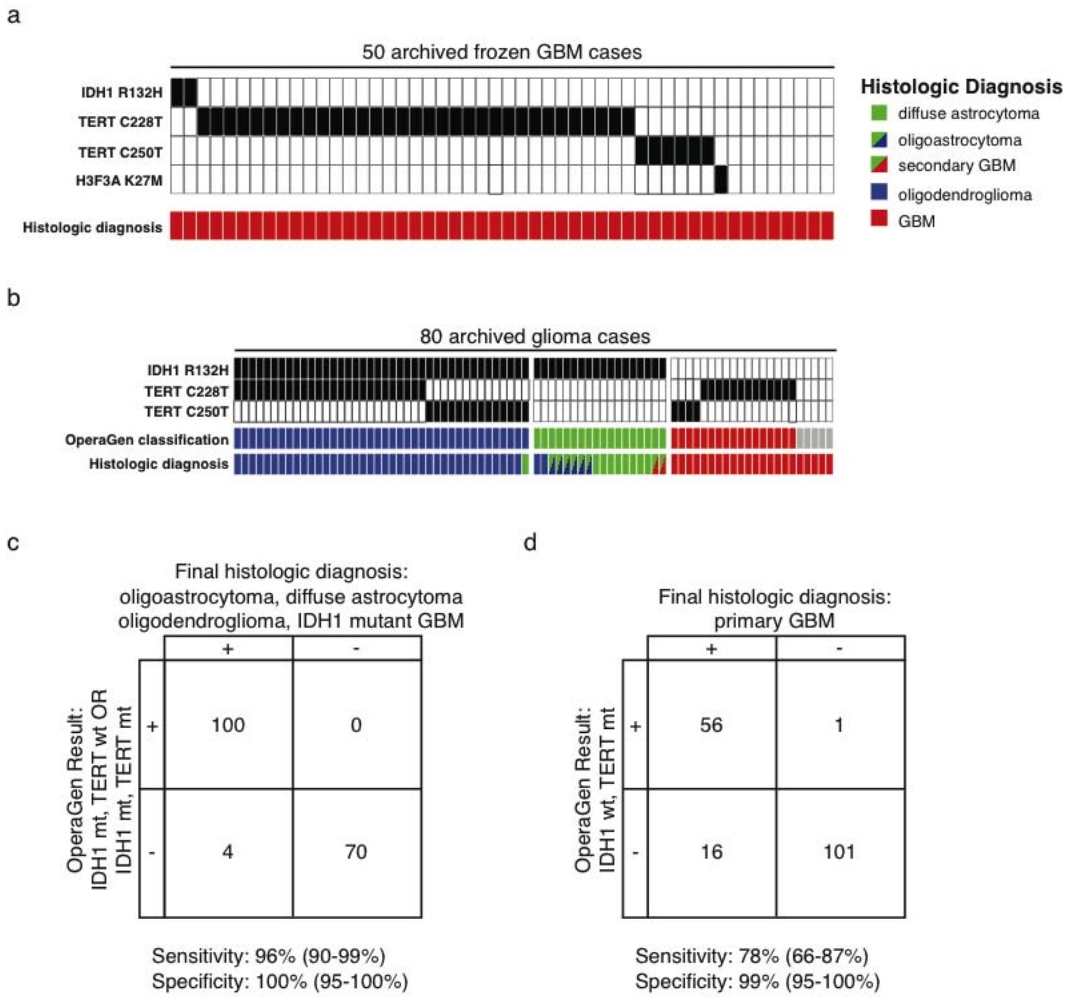

eFigure 9. Sensitivity and specificity analysis of OperaGen results compared to final pathologic diagnosis. (a) Assessment of OperaGen false positive rate in a third cohort representing 50 frozen GBM specimens. Two samples were noted by OperaGen to have IDH1 R132H and 39 samples were noted to have either *TERT* C228T or *TERT* C250T. The prevalence of non-scoring specimens in this cohort is the similar to the ratio of non-scoring GBM specimens in Figure 1a ($p > 0.05$ by Fisher's exact test). (b) Expanded heatmap from Figure 1a demonstrating individual IDH1 R132H, *TERT* C228T and *TERT* C250T mutations for each glioma specimen. OperaGen sensitivity and specificity for predicting (b) oligodendrogliomas, diffuse astrocytomas, oligoastrocytomas or *IDH1* mutant glioblastomas or (d) primary glioblastoma with 95% confidence intervals in parentheses.

eFigure 10

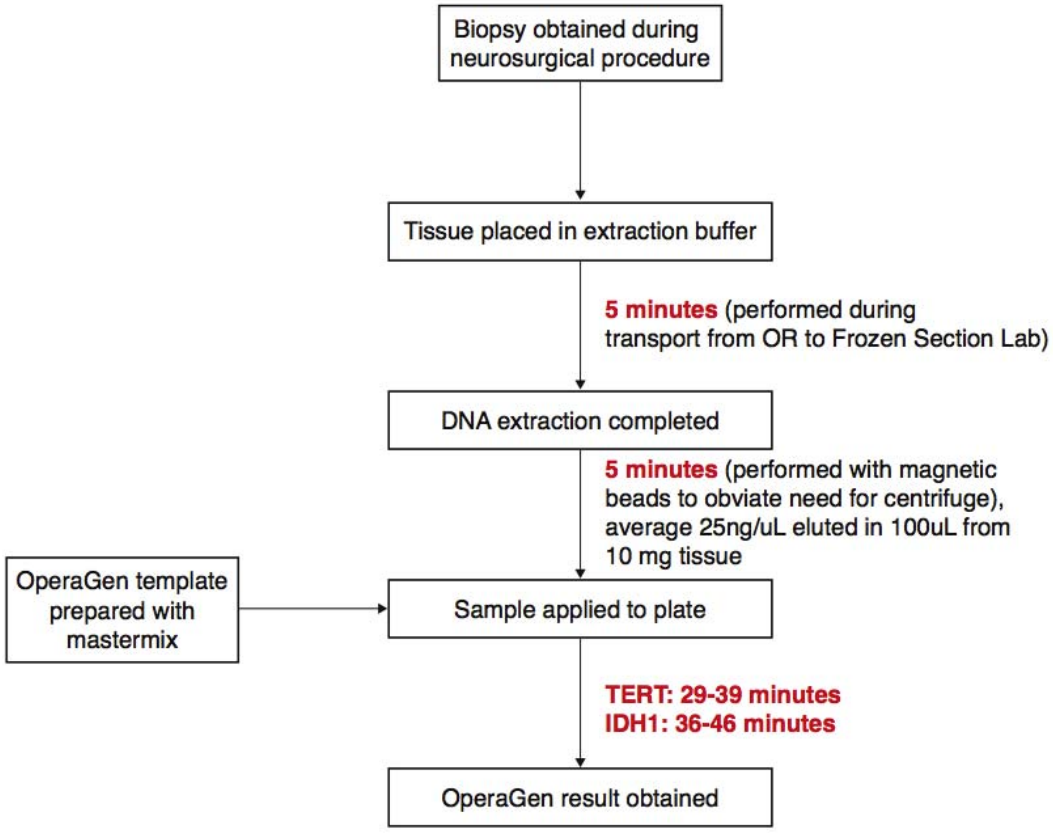

eFigure 10. Proposed workflow of intraoperative OperaGen analysis of biopsy specimen. The specimen would be immediately placed in lysis buffer and incubated at 55˚C en route to the frozen pathology lab. DNA extraction is completed with magnetic beads. This sample is applied to a plate already containing the optimized mastermix to detect *IDH1* R132 variants, *TERT* C228T or *TERT* C250T with respective controls.

eTABLE 1

Gene	sSNV	Forward Primer Sequence (5' -3')	Reverse Primer Sequence (5' -3')	5' Nuclease Probe Sequence (Exiqon)	PNA Blocker Sequence (PNA Bio)
TERT	C228T	CACGTGCGCAGCAGGACGCAG	CTTCACCTTCCAGCTCCGCCTC	CCCAGCCCC+T+TCCGGGCCC	CCCAGCCCCCTCCGGGCCC
TERT	C250T	CACGTGCGCAGCAGGACGCAG	CTTCACCTTCCAGCTCCGCCTC	CCGACCCC+T+TCCGGGTCCC	CCGACCCCTCCCGGGTCCC
IDH1	R132H	CCGGCTTGTGAGTGGATGGGTAAAACCT	CATTATTGCCAACATGACTTACTTGATCCCC	AGG+T+C+A+T+CAT+GC	AGGTCGTCATGC
IDH1	R132C	CCGGCTTGTGAGTGGATGGGTAAAACCT	CATTATTGCCAACATGACTTACTTGATCCCC	AGG+T+T+G+T+C+ATGC	AGGTCGTCATGC
IDH1	R132G	CCGGCTTGTGAGTGGATGGGTAAAACCT	CATTATTGCCAACATGACTTACTTGATCCCC	AGGT+G+G+T+CAT+GC	AGGTCGTCATGC
IDH1	R132S	CCGGCTTGTGAGTGGATGGGTAAAACCT	CATTATTGCCAACATGACTTACTTGATCCCC	AGGT+A+G+T+CA+T+GC	AGGTCGTCATGC
IDH1	R132S	CCGGCTTGTGAGTGGATGGGTAAAACCT	CATTATTGCCAACATGACTTACTTGATCCCC	AGG+T+C+T+T+CAT+GC	AGGTCGTCATGC

eTable 1. List of primers, detection probes and modified oligonucleotide blockers. Modified locked nucleic acids are indicated by a preceeding "+".

eTABLE 2

Case ID	Frozen histologic diagnosis	Final histologic diagnosis
Non-glioma 1	Fragments of gray and white matter with mixed perivascular inflammatory infiltrates. No evidence of malignancy	Multiple Sclerosis (subsequent Autopsy)
Non-glioma 2	Fragments of cortex, mildly hypercellular gliotic brain, lesional tissue with chronic inflammation and macrophages	Tumefactive MS (subsequent Autopsy)
Non-glioma 3	Small fragment of cortex and white matter with scattered reactive astrocytes, white matter with active demyelination	Tumefactive MS (subsequent Autopsy)
Non-glioma 4	Destructive lesion with surrounding acute ischemic changes and inflammatory cell infiltrates consisting primarily of lymphoid cells and macrophages; some loss of myelin - Ddx infarction, infectious process, possibly acute multiple sclerosis or mitochondrial disorder with vascular involvement	Multiple Sclerosis (preoperative concern for glioma)
Non-glioma 5	Neocortex with disorganization of ganglion cells, atypical clustering of ganglion cells and rare vacuolated, binucleated and balloon-like cells consistent with forcal cortical dysplasia	Focal Cortical Dysplasia (preoperative suspicion for focal cortical dysplasia)
Non-glioma 6	Brain parenchyma with multiple areas of acute and chronic hypoxic/ischemic injury, dysplastic and disorganized neurons and prominent gliosis	Cortical Dysplasia (based on further history, prior biopsy)
Non-glioma 7	Dense fibrous tissue with no diagnostic abnormality; fragments of gray and white matter with diffuse reactive astrocytosis, lymphocytes and microglia;	presumed CNS vasculitis; Dx unknown
Non-glioma 8	Diffuse gliosis; grey and white matter with focus suspicious for dysplastic neuronal heterotopia	Seizure disorder; resection of seizure focus
Non-glioma 9	Gliosis and hemosiderin-laden macrophages; gliosis, ischemic necrosis; Intracranial dural AV Fistula	AV dural Fistula
Non-glioma 10	Gliotic cerebral cortex with abnormal subarachnoid and intraparenchymal vessles	ICH w/ AVM; seizure disorder
Non-glioma 11	Brain with hypercellularity and atypical cells	secondary CNS Lymphoma; DLBCL (based on subsequent biopsy off steroids)
Non-glioma 12	Malignant tumor, probably metastatic. Rule out lymphoma	Diffuse large B-cell lymphoma
Non-glioma 13	Brain with reactive gliosis with moderate cytologic atypica and scattered macrophages; no evidence of high grade tumor; favor low grade tumor vs malformative lesion vs prior destructive lesion	Demyelination
Non-glioma 14	White matter with reactive gliosis and increased cellularity around several vessels; the specimen is not diagnostic for tumor	Gliosis/inflammation

eTable 2. List of non-glioma biopsies analyzed by OperaGen. Fourteen non-glioma biopsy specimens were analyzed for *IDH1* and *TERT* promoter variants by OperaGen. None of these were noted to be positive for variants in either gene.

eTABLE 3

Sample Code	Number of biopsies obtained	Intraoperative histologic interpretation	Final histologic interpretation
BX1	7	gray and white matter with rare atypical nuclei of uncertain significance and some reactive changes	WHO grade II astrocytoma
BX2	4	atypical glial nuclei and reactive astrocytes, favor glioma	WHO grade II astrocytoma
BX3	2	cerebral cortex and white matter with minimal hypercellularity	WHO grade II astrocytoma
BX4	2	hypercellular brain tissue WHO grade II astrocytoma	WHO grade II astrocytoma
BX5	4	suspicious for infiltrating glioma WHO grade II astrocytoma	WHO grade II astrocytoma
BX6	4	gray and white matter with one gliotic focus, not diagnostic	WHO grade II oligoastrocytoma
BX7	3	slight hypercellularity and slightly reactiv WHO grade II oligoastrocytoma	WHO grade II oligoastrocytoma
BX8	3	white matter with minimal hypercellularity WHO grade II oligoastrocytoma	WHO grade II oligoastrocytoma
BX9	2	hypercellular brain tissue with scattered atypical cells and reactive astrocytes and lymphocytes; favor reactive process but can't rule out tumor on frozen	WHO grade II oligodendroglioma
BX10	2	diagnostic tissue; favor hematopoietic/lymphoid proliferation	WHO grade II oligodendroglioma
BX11	6	hypercellular brain with atypical cells; could represent infiltrating glioma or lymphoma but solid tumor is not present	WHO grade III astrocytoma
BX12	3	hypercellular gray and white matter with reactive astrocytes and a few atypical nuclei	WHO grade III astrocytoma
BX13	3	hypercellular white matter with scattered atypical cells, reactive astrocytes and myxoid material GBM	GBM
BX14	2	suspicious for lymphoma GBM	GBM

eTable 3. Intraoperative histologic analysis of 14 stereotactic glioma biopsies. The intraoperative histologic analysis and final histologic diagnosis are presented for the 14 biopsy cases presented in Figure 2b (preserving the order from left to right). The number of biopsy cores obtained for each patient is listed in the second column.